Journal of Medicinal Chemistry

pubs.acs.org/jmc

Article

Role of Chain Length and Degree of Unsaturation of Fatty Acids in the Physicochemical and Pharmacological Behavior of Drug−Fatty Acid Conjugates in Diabetes

Arihant Kumar Singh, Kishan S. Italiya, Saibhargav Narisepalli, Deepak Chitkara, and Anupama Mittal*

Cite This: https://doi.org/10.1021/acs.jmedchem.1c00391

Read Online

ACCESS | Metrics & More | Article Recommendations | Supporting Information

ABSTRACT: Several drug−fatty acid (FA) prodrugs have been reported to exhibit desirable physicochemical and pharmacological profile; however, comparative beneficial effects rendered by different FAs have not been explored. In the present study, four different FAs (linoleic acid, oleic acid, palmitic acid, and α-lipoic acid) were selected based on their chain length and degree of unsaturation and conjugated to Lisofylline (LSF), an antidiabetic molecule to obtain different drug−FA prodrugs and characterized for molecular weight, hydrophobicity, purity, self-assembly, and efficacy *in vitro* and *in vivo* in type 1 diabetes model. Prodrugs demonstrated a 2- to 6-fold increase in the plasma half-life of LSF. Diabetic animals treated with prodrugs, once daily for 5 weeks, maintained a steady fasting blood glucose level with a significant increase in insulin level, considerable restoration of biochemical parameters, and preserved β-cells integrity. Among the different LSF-FA prodrugs, LSF-OA and LSF-PA demonstrated the most favorable physicochemical, systemic pharmacokinetic, and pharmacodynamic profiles.

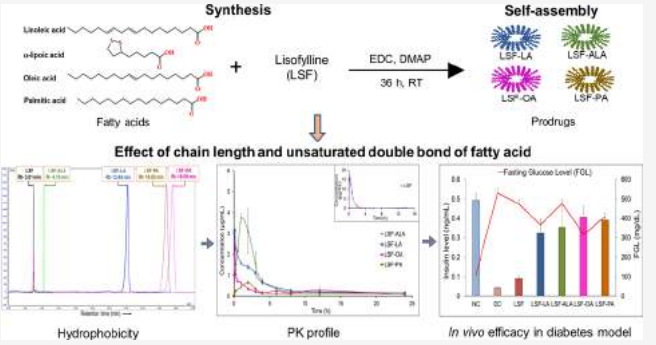

INTRODUCTION

Diabetes mellitus (DM) is a widespread chronic metabolic disorder classified into autoimmune insulin-dependent type 1 DM (T1DM) and non-insulin-dependent type 2 DM (T2DM) caused by insulin resistance resulting in a high blood glucose level. T1DM develops owing to proinflammatory cytokine-mediated β-cell dysfunction and inflammation in the islet of Langerhans of pancreas leading to activation of macrophages and release of inflammatory Th1 lymphocytes and cytotoxic T-cells, which lead to chronic complications after a few years.[1] Lisofylline (LSF) is a broad-spectrum drug bearing significant clinical utility in preventing both T1DM and T2DM by suppressing autoimmunity and retaining insulin secretory function of β-cells in the presence of inflammatory cytokines. Chemically, LSF is a hydrophilic drug molecule (280.328 Da) having free hydroxyl group in its structure, making it viable for rapid metabolism into pentoxifylline (PTX) resulting in a short half-life (30−40 min). Numerous studies have been reported, wherein therapeutic moieties are conjugated to a lipidic biomolecule, i.e., phospholipids, glycerides, or fatty acids (FAs) to improve their efficacy and permeability or/and oral bioavailability.[2−7] A well-known marketed formulation, Liraglutide, is a myristic acid (short-chain FA) derivative of glucagon-like peptide-1 (GLP-1) and has shown improved efficacy and plasma half-life from 2 min to 15 h. It enhanced the binding efficiency of the prodrug with albumin, improving its retention in the body.[8]

FAs are obtained exogenously from various sources like plants, animals, and marine organisms and are also endogenously synthesized in our body. They generally contain a linear chain of carbon atoms with a reactive carboxyl end group that can form a strong ester or amide bond with any drug having α-hydroxyl or amine group.[9−11] These are classified as saturated and unsaturated FAs (SFAs and USFAs), of which USFAs are further designated according to the position of double bonds like n-3, -6, and -9 (where n indicates the number of carbon atoms after double bond). Long-chain monounsaturated and polyunsaturated fatty acids (MUFAs contain one double bond; PUFAs contain two or more double bonds) play an important role in cholesterol metabolism, blood clotting, and immune system regulation. FAs also constitute an important component of most of the biological phospholipidic membranes.

Received: March 4, 2021

Scheme 1. Reaction Scheme of the Synthesized Prodrugs with Different Fatty Acids and LSF

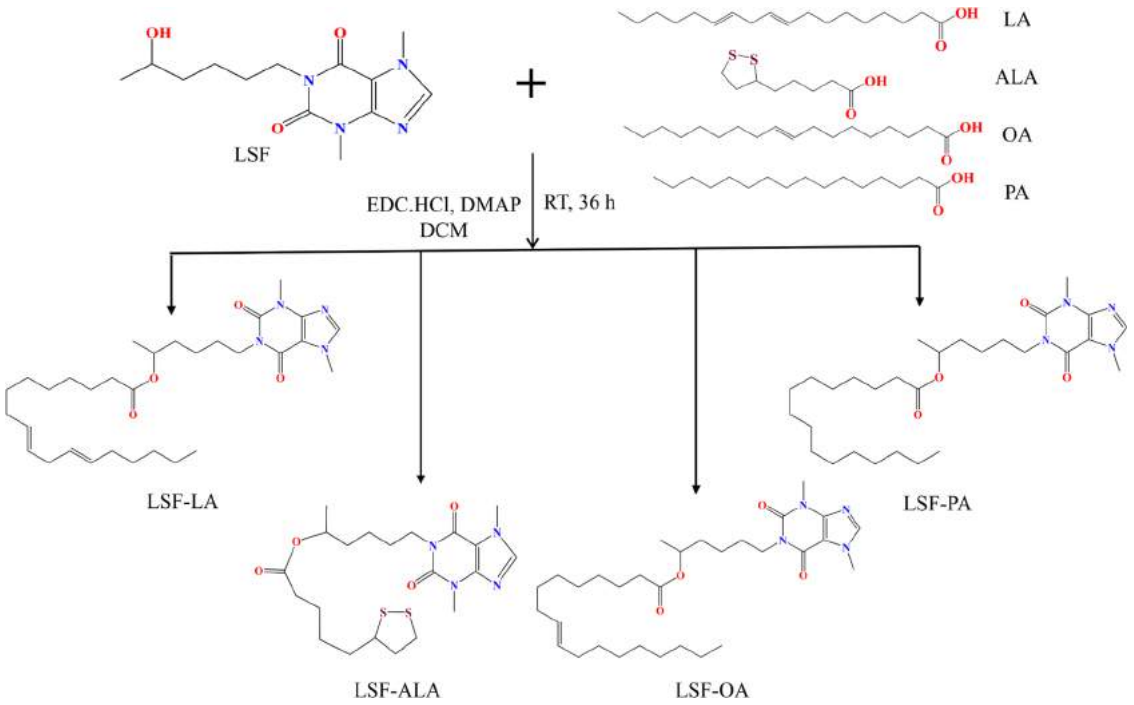

Table 1. HPLC and HR-MS Analyses of the synthesized LSF and LSF Prodrugs

S. No.	drug/prodrugs	molecular formula	% yield	retention time (R_t, min)	purity (%)	expected mass (g/mol)	$(M + H)^+$ peak (g/mol)
1	free LSF	$C_{13}H_{20}N_4O_3$	92	6.21	99.7	280.1535	281.1551
2	LSF-ALA	$C_{21}H_{32}N_4O_4S_2$	52	4.19	95.1	468.1865	469.1933
3	LSF-LA	$C_{31}H_{32}N_4O_4$	41.91	13.84	98.4	542.3832	543.3994
4	LSF-PA	$C_{29}H_{50}N_4O_4$	55.75	18.82	98.	518.3832	519.3889
5	LSF-OA	$C_{31}H_{52}N_4O_4$	49.25	19.69	95.3	544.3989	545.4044

Previously, our group reported LSF-linoleic acid (LSF-LA) prodrug, which showed a significant increase in the half-life of LSF by 5.7-fold and reduced the preclinical dose from 25 to 15 mg/kg and frequency from twice daily to once daily. The prodrug exhibited self-assembly and formed nanosized micelles and demonstrated improved antidiabetic efficacy.[12] In this study, different FAs have been explored for conjugation to LSF to evaluate the effect of carbon chain length and double bonds present in their structures. Further to reduce the solubility of hydrophilic LSF and to enhance its efficacy and bioavailability, FAs belonging to different classes like LA (omega-6), OA (omega-9), PA (conjugated fatty acid), and ALA (functional fatty acid) were selected to form prodrugs with LSF with increased lipophilicity, wherein LSF-α-lipoic acid (LSF-ALA), LSF-palmitic acid (LSF-PA), LSF-oleic acid (LSF-OA), and LSF-LA were synthesized, characterized, and analyzed for their chemical structure and self-assembling behavior. The stability and release of free LSF from these prodrugs in plasma were also studied. The cell viability in the presence of FAs and synthesized prodrugs was confirmed in MIN-6 cells (originated from insulinoma cells of mouse) under normal as well as under inflammatory conditions similar to those observed in diabetes. All of the prodrugs were studied for their systemic pharmacokinetic behavior in Wistar rats at a single dose of ~15 mg/kg of free LSF. The antidiabetic activity was monitored by administering the prodrugs by intraperitoneal (i.p.) route daily for 35 days in streptozotocin (STZ)-induced T1DM rat model. Post-treatment, evaluation of efficacy was carried out by measuring blood glucose level, plasma insulin level, and biochemical parameters. The excised pancreatic tissues of the experimental animals were studied for histopathological changes by hematoxylin and eosin (H&E) staining and expression of CD4+ and CD8+ T-cells.

RESULTS

Synthesis and Characterization of LSF and LSF−Fatty Acid Prodrugs. LSF was successfully synthesized with >98% purity as determined by high-performance liquid chromatography (HPLC, Thermo Fisher Scientific), and a complete reduction of the ketone group present in PTX was seen, giving a high % yield. LSF-FA prodrugs were then successfully synthesized (Scheme 1) and purified by flash chromatography using varying ratios of hexane and ethyl acetate as mobile phase for different prodrugs (Table S1) with approximately 50% yield except for LSF-LA (41.91% yield) (Table 1). The physical appearance of the purified prodrugs was quite different from each other, wherein LSF-LA and LSF-OA were colorless and semisolid, but LSF-PA was white and LSF-ALA was light yellow; both were solid in nature. LSF and its FA prodrugs exhibited the following attributes when characterized by different spectroscopic and analytical techniques.

^{1}H nuclear magnetic resonance spectroscopy (proton NMR; Bruker CMC 400 MHz, $CDCl_3$) of the synthesized LSF drug showed a peak at a chemical shift value of 3.75 ppm (−CH−OH) corresponding to the hydroxyl group in the side chain of LSF formed by the reduction of ketone group of PTX. Further,

https://doi.org/10.1021/acs.jmedchem.1c00391
J. Med. Chem. XXXX, XXX, XXX−XXX

the successful conjugation of FA with LSF was confirmed, wherein all of the prodrugs exhibited a peak at 4.9 ppm corresponding to the formation of an ester (−CH−COO⁻) group and removal of peak for the hydroxyl proton (−CH−OH) signifying a complete reaction between LSF and FAs and absence of any free drug in the purified products (Figures S1−S6). In HPLC analysis, lab-synthesized LSF exhibited a retention time (R_t) of 6.21 min, indicating its hydrophilic nature, and no additional peak was detected in the chromatogram of LSF, indicating the absence of any impurity/reaction byproducts (Figure S7).[13] The spectrum of the synthesized LSF was similar to that of the commercially available LSF (Cayman chemical). For quantification of prodrugs, HPLC analysis was carried out as mentioned in the below-validated analytical method. Here, LSF showed an R_t value of 3.01 min, whereas the prodrugs showed an increased R_t compared to the drug alone (Figure S8). Among all, the minimum R_t was observed for LSF-ALA (4.19 min) followed by other prodrugs as shown in Table 1, indicating enhanced hydrophobicity of the prodrugs. All of the prodrugs were obtained with a purity of >95% with a negligible amount of free LSF present in the final product (Figures S9−S12). A peak corresponding to any other impurity was also not observed in any of the chromatograms. High-resolution mass spectroscopy (HR-MS, Agilent Technologies 6545 Q-TOF LC/MS) showed $(M + H)^+$ ion peaks (expected mass of the drug/prodrug + mass of ^1H) (Figure S13), which were found to be closely matching with the molecular formula of the respective prodrug and exactly calculated mass of LSF/prodrugs (Table 1). In Fourier transform infrared (FT-IR) spectroscopy (Bruker, ALPHA), the LSF spectra showed a peak at 3380 cm^{-1} corresponding to the −CH−OH group that was absent in the spectra of all of the prodrugs as it was consumed in ester bond (−C═O) formation as depicted by the presence of the −COOH peak at 1700−1650 cm^{-1} in the FTIR spectra of the prodrugs (Figure S14).

Analytical Method Development for Prodrugs. FAs have short and long carbon chains with/without double bonds, resulting in variation in their hydrophobicity, and therefore, only the retention time of the different prodrugs was different in the HPLC analysis (Table 1). The polynomial regression for the calibration plots showed a good linear relationship with correlation coefficient (R^2) for LSF-ALA and LSF-OA, which was found to be >0.9995 over the concentration range of 1−100 μg/mL. The methods were also found to be selective for the analytes (Table 2). The limit of detection (LOD) and limit of quantification (LOQ) were 13 and 41 ng/mL for LSF-ALA and 52 and 159 ng/mL for LSF-OA, respectively. Results of method validation are provided in the Supporting Information (Tables S2 and S3).

Table 2. Chromatographic Conditions for Analytical Method Development of LSF-FA Prodrugs

chromatographic conditions	
instrument	Ultimate HPLC 3000, Thermo Fisher Scientific
column	Inertsil ODS (C18), (250 mm × 4.6 mm, 5 μm)
mobile phase (Isocratic mode)	acetonitrile/acetate buffer pH 3.5 (95:05 % v/v)
flow rate	1 mL/min
column temperature	30 ± 0.5 °C
injection volume	20 μL
wavelength	273 nm

Stability of Prodrugs in Plasma. Due to the conjugation of LSF to FAs, its stability in rat plasma increased and the prodrugs released LSF in a sustained manner for 72 h, wherein LSF-ALA exhibited a maximum release of 100% in 72 h followed by other prodrugs (Figure 1).

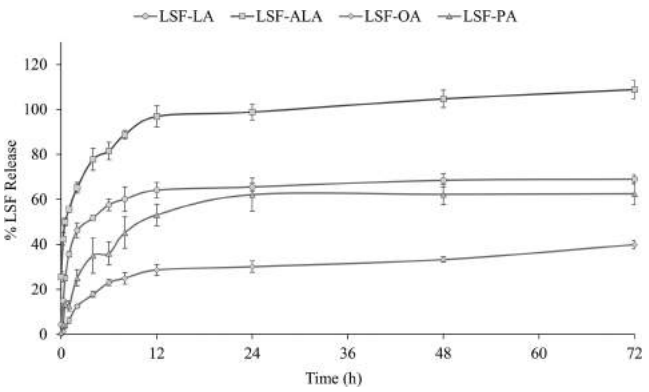

Figure 1. Stability of LSF prodrugs and the rate of release of free LSF from the prodrugs in the rat plasma. Data represent mean (n = 3) ± SD.

Self-Assembly of Prodrugs. These prodrugs are amphiphilic in nature as these comprise hydrophilic (LSF) and hydrophobic components (FAs) in a 1:1 ratio (on a mole basis), which imparts self-assembling property to them, enabling the formation of micelles in the presence of water. The self-assembled micelles were characterized for particle size and ζ-potential using a Malvern dynamic light scattering system (Table 3). The micelle size ranged from 70.4 to 170.5 nm, and the ζ-potential values ranged from −4.3 to −22.6 mV for different prodrugs. For confirming the self-assembly of micelles, the CMC value was obtained for each of the prodrugs and was found to be in range of 0.81−7.58 μg/mL (Figure 2A).

Estimation of Aggregation Number (N_{agg}). N_{agg} was determined after estimating the concentration of micelles (M) by the steady-state fluorescence, and the intensities were compared with and without quencher. So, the decrease in the intensity of pyrene with prodrug micelles in the presence of various concentrations of cetylpyridinium chloride (CPC) (quencher) was recorded. A straight line was obtained when a graph was plotted between $\ln(F_0/F_Q)$ and Q (concentration of quencher in micelles), where M was determined by the slope of the graph using eq 1 and N_{agg} was calculated using eq 2 (Figure 2B).

Protein Interaction of Prodrugs with Bovine Serum Albumin (BSA). This study was performed to check the interaction of protein with prodrugs by the fluorescence quenching method, wherein the emission spectra of BSA were recorded before and after interaction of BSA with free LSF and prodrugs. A decrease in the relative intensity of BSA with an increase in the concentration of prodrugs was observed, revealing an interaction between BSA and prodrugs. A bathochromic peak shift was observed only in the case of LSF-PA, which itself showed fluorescence (Figure 3). After plotting the graph of $\log(F_0 - F_Q)/F_Q$ and $\log Q$, the binding constant K_b and number of binding sites (n) present on BSA

https://doi.org/10.1021/acs.jmedchem.1c00391
J. Med. Chem. XXXX, XXX, XXX−XXX

Table 3. Characterization of Self-Assembled LSF−Fatty Acid Micelles

S. No.	prodrugs	particle size (nm)	PDI	ζ potential	CMC (μg/mL)	LSF (μg/mL equivalent to 20 μM)	N_{agg}	K_b (L/mol)	n
1	LSF-ALA	170.5	0.257	−13.0	6.31	9.36	47	2.05×10^4	1.18
2	LSF-LA	92.67	0.326	−22.6	0.81	10.85	52	2.70×10^4	1.03
3	LSF-PA	71.74	0.268	−4.3	7.4	10.37	69	5.55×10^4	0.85
4	LSF-OA	70.4	0.232	−15.6	7.58	10.88	61	6.34×10^4	0.92

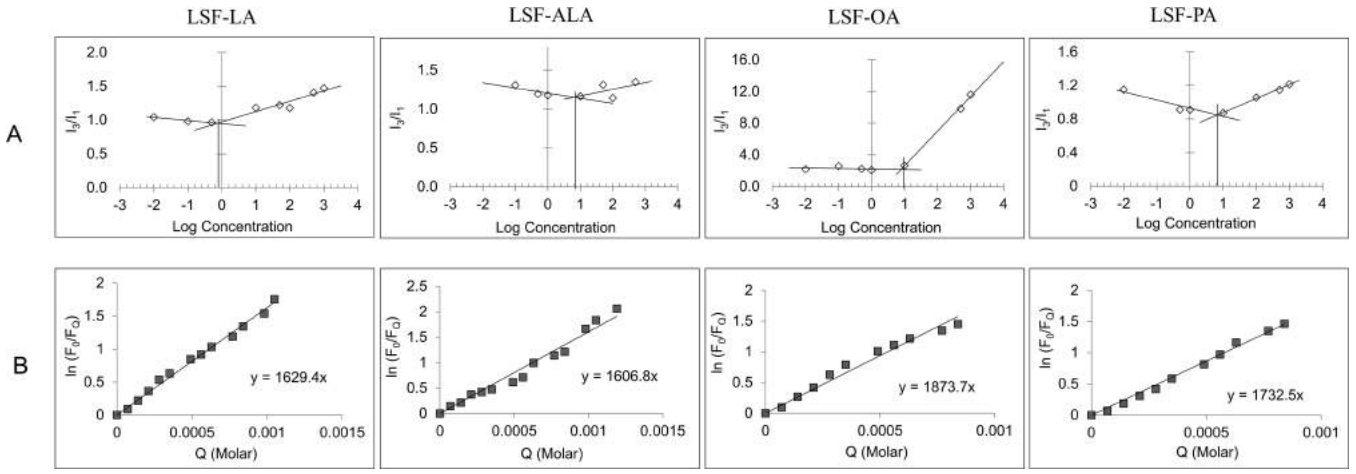

Figure 2. Study of the self-assembling nature of LSF prodrugs by (A) critical micelle concentration (CMC) and (B) micelles aggregation number.

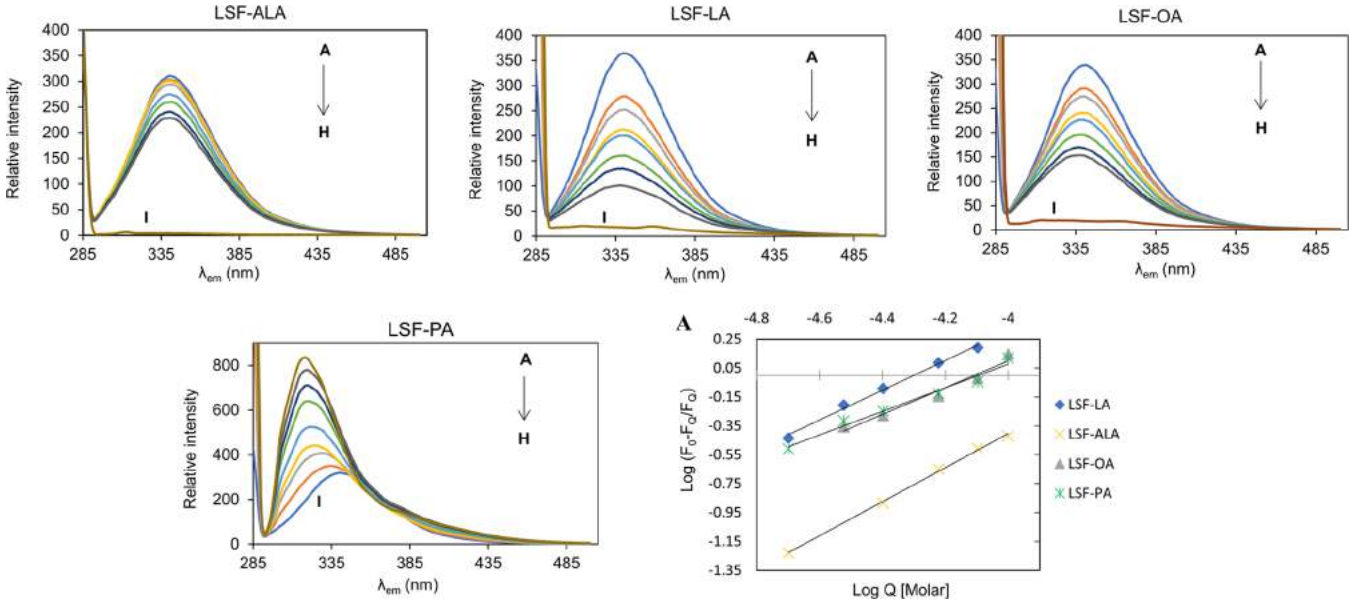

Figure 3. Protein interaction study between LSF prodrugs and BSA. Emission spectra of BSA (λ_{ex} = 280 nm) at 2.0 μM concentration in the presence of different concentrations of prodrug micelles, that is, 0, 10, 20, 30, 40, 60, 80, and 100 μM, corresponding to curves (A−H). Plot I corresponds to the emission spectrum of respective prodrug micelle only (500 μM). (A) Plot of $\log(F_0 - F_Q/F_Q)$ against $\log(Q)$ at different concentrations of the prodrugs at room temperature.

were determined (Table 3). The K_b and n values for free LSF were estimated to be 6.32×10^4 and 1.16, respectively.

***In Vitro* Studies of Prodrugs.** *Hemocompatibility Study.* To understand if the micelles can cause hemolysis during systemic circulation, % hemolysis was calculated. Hemolysis exhibited by the different prodrugs was very less compared to the lysis caused by the positive control (Triton X) (Figure 4A,B).

Cell Internalization of Prodrug Micelles. As micelles are nanosized systems, the prodrug micelles exhibited a higher cell uptake into MIN-6 cells compared to the free drug after 6 h, wherein LSF was analyzed in the incubated media, washings, as well as after lysis of the cells. We found that 56 ng of LSF was present in cell lysates treated with LSF-OA after 6 h, followed by LSF-LA and LSF-PA prodrugs (Figure 4C).

Cell Viability under Normal and Inflammatory Conditions. Under normal cell culture conditions, all of the prodrugs, free drug, and FAs exhibited no cell death after 48 h, confirming that the synthesized prodrugs of LSF are nontoxic to the cells (Figure 4D). As seen in Figure 4E, upon exposure to the cytokine (cyt)-mediated inflammatory conditions, a drastic reduction in cell viability was observed in all of the

https://doi.org/10.1021/acs.jmedchem.1c00391
J. Med. Chem. XXXX, XXX, XXX−XXX

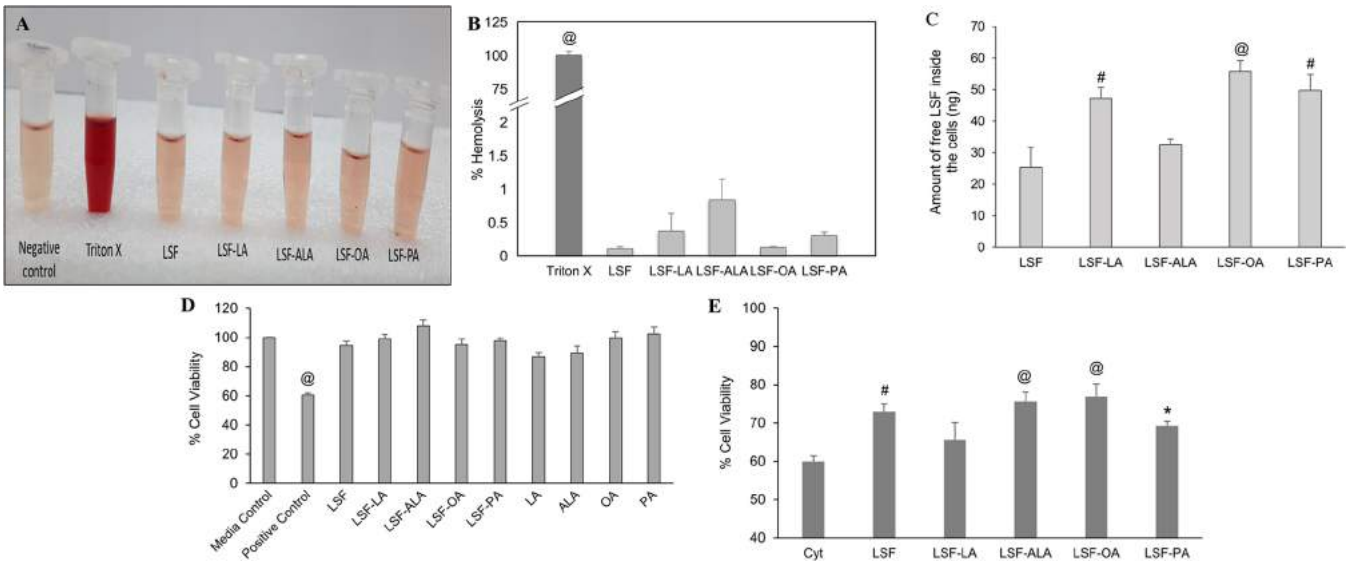

Figure 4. *In vitro* evaluation of the LSF prodrugs. (A, B) *In vitro* hemocompatibility study $^{@}$Triton X *vs* all ($^{@}P < 0.0001$), (C) cell uptake study in MIN-6 cells after 6 h of incubation $^{@}$LSF *vs* LSF-OA ($^{@}P < 0.0001$); $^{\#}$LSF *vs* LSF-LA and LSF-PA ($^{\#}P < 0.001$), (D) cytotoxicity study of FAs, LSF (20 μM), and prodrugs (~20 μM free LSF) under normal conditions $^{@}$Positive control *vs* all groups ($^{@}P < 0.0001$), and (E) cell viability in the presence of cytokine induced inflammation $^{@}$Cyt *vs* LSF-ALA and LSF-OA ($^{@}P < 0.0001$); $^{\#}$Cyt *vs* LSF ($P < 0.001$); *Cyt *vs* LSF-PA ($^{*}P < 0.05$). *In (C), all of the bars correspond to the amount of free LSF released from the corresponding prodrugs shown on the *x*-axis.

Table 4. Systemic Pharmacokinetic Study of LSF (15 mg/kg; i.v. dose) and LSF Prodrug (30 mg/kg; i.v. Dose) Administered in Rat and Analyzed by the Noncompartmental Method (Mean ± SEM)

	LSF	LSF-LA	LSF-ALA	LSF-OA	LSF-PA
C_0 (ng/mL)[a]	16 395.65 ± 1630.78	4902.86 ± 3223.37	4117.86 ± 588.65	4747.3 ± 3028.56	266.75 ± 110.19
$t_{1/2}$ (h)	0.752 ± 0.03	3.12 ± 0.29	1.26 ± 0.13	4.44 ± 0.47	3.59 ± 0.51
K_e (1/h)	0.924 ± 0.04	0.23 ± 0.02	0.51 ± 0.06	0.16 ± 0.02	0.17 ± 0.01
AUC_{0-t} (ng h/mL)	14 692.73 ± 603.55	16 157.94 ± 5437.84	13 467.82 ± 1538.58	6107.96 ± 1322.07	3491.96 ± 145.55
AUC_{0-OO} (ng h/mL)	14 738.52 ± 590.77	16 984.11 ± 5365.74	13 838.8 ± 1439.5	6635.59 ± 1270.95	3887.79 ± 268.31
$AUMC_{0-t}$ (ng h/mL)	12 068.34 ± 1247.91	77 115.13 ± 13 161.58	67 512.96 ± 3282.77	30 549.55 ± 7409.28	29 926.06 ± 1339.38
$AUMC_{0-OO}$ (ng h/mL)	12 797.01 ± 1278.92	98 737.84 ± 18 277.97	77 295.34 ± 5430.21	43 158.66 ± 14430.4	24 806.43 ± 3905.12
MRT (h)	0.818 ± 0.06	6.55 ± 0.55	5.16 ± 0.67	7.91 ± 0.93	9.07 ± 0.33
V_d (mL/kg)	961.55 ± 79.16	2587.82 ± 558.86	1769.5 ± 395	14 974.4 ± 1588.02	13774.62 ± 2501.16
CL (mL/(h kg))	1020.9 ± 39.46	634.05 ± 191.99	951.84 ± 107.22	2415.3 ± 407.29	3894.14 ± 260.65

[a]The concentrations refer to the free LSF released in plasma from the prodrugs.

samples. However, the presence of LSF prodrugs with the cells under these conditions significantly preserved their viability in comparison to the control cells (in media alone).

In Vivo Studies of Prodrugs. Systemic Pharmacokinetic Study. The noncompartmental estimation of pharmacokinetic (PK) parameters showed that the conjugation of LSF increased the half-life of LSF by 2- to 6-fold (from 0.752 ± 0.03 to 4.44 ± 0.47 h), and the apparent volume of distribution of prodrugs also increased from 3- to 15-fold. The mean residence time (MRT) of prodrug elevated to 9 h compared to 0.8 h for free LSF. The clearance values of LSF-LA and LSF-ALA prodrugs were found to be lower than that of free LSF but found to be much higher in LSF-OA and LSF-PA as shown in Table 4 (Figure 5).

In Vivo Efficacy Studies in STZ-Induced T1D Model. The LSF-FA self-assembled micelles were administered once daily intraperitoneally at a dose of 30 mg/kg (~15 mg/kg of LSF) over a period of 5 weeks and compared with free LSF dosed at 15 mg/kg, once daily. In this study, fasting glucose levels (FGL) of animals (mg/dL) were recorded every week. An overall FGL level at 3rd and 5th week exhibited decreased FGL levels. The diabetic control group (DC) showed a significant

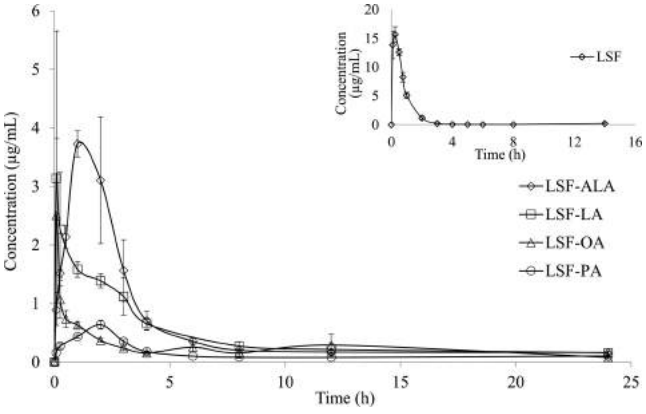

Figure 5. Systemic pharmacokinetic study of LSF and LSF prodrugs in Wistar rats, IV administration. Each point represents mean ($n = 4$) ± SD at ~15 mg/kg dose of free LSF.

increase in FGL level (555.5 ± 22.73 mg/dL) compared to normal control (NC) animals (106.25 ± 4.77 mg/dL) as no treatment was given to this group except for saline. Free LSF

https://doi.org/10.1021/acs.jmedchem.1c00391
J. Med. Chem. XXXX, XXX, XXX−XXX

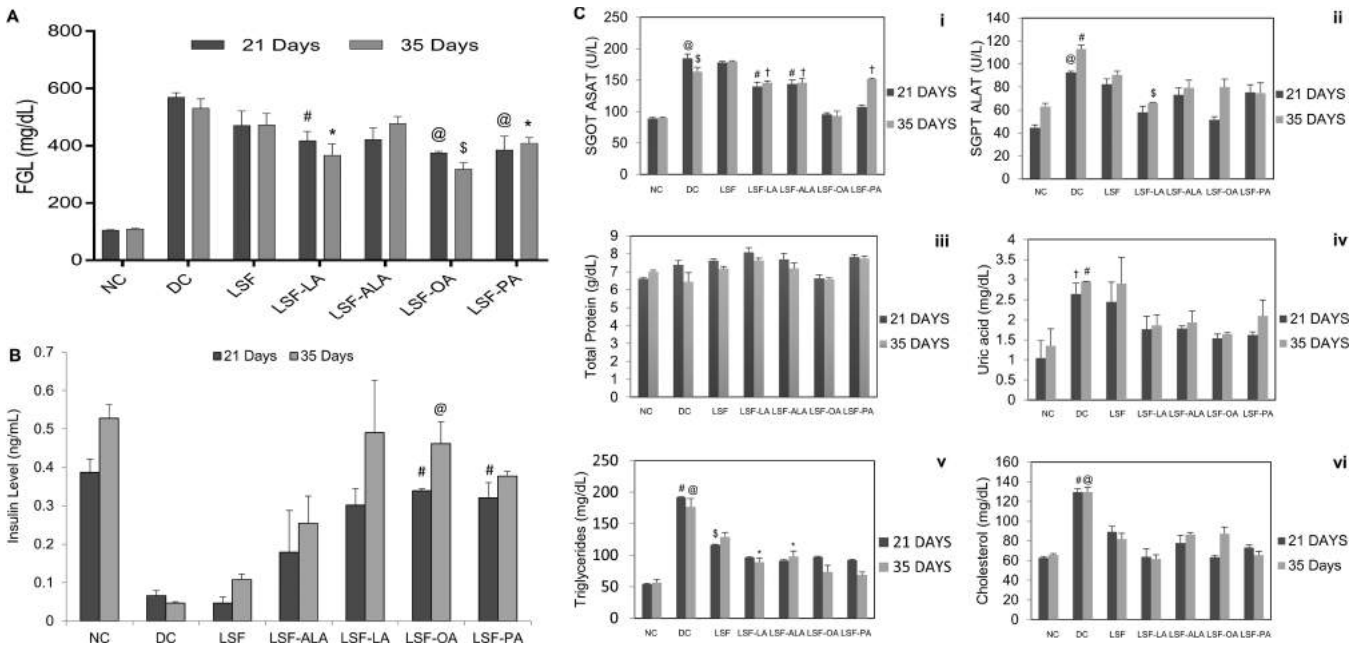

Figure 6. *In vivo* antidiabetic activity of the LSF prodrugs evaluated in an STZ-induced diabetic model. (A) Fasting blood glucose levels after 35 days $^{\$}$DC *vs* LSF-OA ($^{\$}P < 0.005$); $^{@}$DC *vs* LSF-OA and LSF-PA; *DC *vs* LSF-LA and LSF-PA ($^{@}$*$P < 0.01$); $^{\#}$DC *vs* LSF-LA ($^{\#}P < 0.05$). (B) Serum insulin level $^{\#}$DC *vs* LSF-OA and LSF-PA; $^{@}$DC *vs* LSF-OA ($^{\#@}P < 0.05$). (C) Biochemical analysis of plasma (i) SGOT $^{@}$DC *vs* LSF-OA and LSF-PA; $^{\$}$DC *vs* LSF-OA ($^{@\$}P < 0.005$); $^{\#}$DC *vs* LSF-LA and LSF-ALA ($^{\#}P < 0.01$); †DC *vs* LSF-LA, LSF-ALA, and LSF-PA ($^{\dagger}P < 0.05$), (ii) SGOT $^{@}$DC *vs* LSF-LA and LSF-OA, $^{\$}$DC *vs* LSF-LA ($^{@\$}P$<0.005); $^{\#}$DC *vs* LSF-ALA, LSF-OA, and LSF-PA ($^{\#}P < 0.05$), (iii) total protein (nonsignificant), (iv) uric acid †DC *vs* LSF-LA, LSF-ALA, LSF-OA, and LSF-PA ($^{\dagger}P < 0.01$); $^{\#}$DC *vs* LSF-LA, LSF-ALA, and LSF-OA ($^{\#}P < 0.005$), (v) triglycerides $^{@}$DC *vs* LSF-LA, LSF-ALA, LSF-OA, and LSF-PA; $^{\#}$DC *vs* LSF-OA and LSF-PA ($^{@\#}P < 0.001$); $^{\$}$DC *vs* LSF; *DC *vs* LSF-LA and LSF-ALA ($^{\$}$*$P < 0.05$), (vi) cholesterol $^{\#}$DC *vs* LSF-LA and LSF-OA ($^{\#}P < 0.005$); $^{@}$DC *vs* LSF-LA and LSF-OA ($^{@}P < 0.01$).

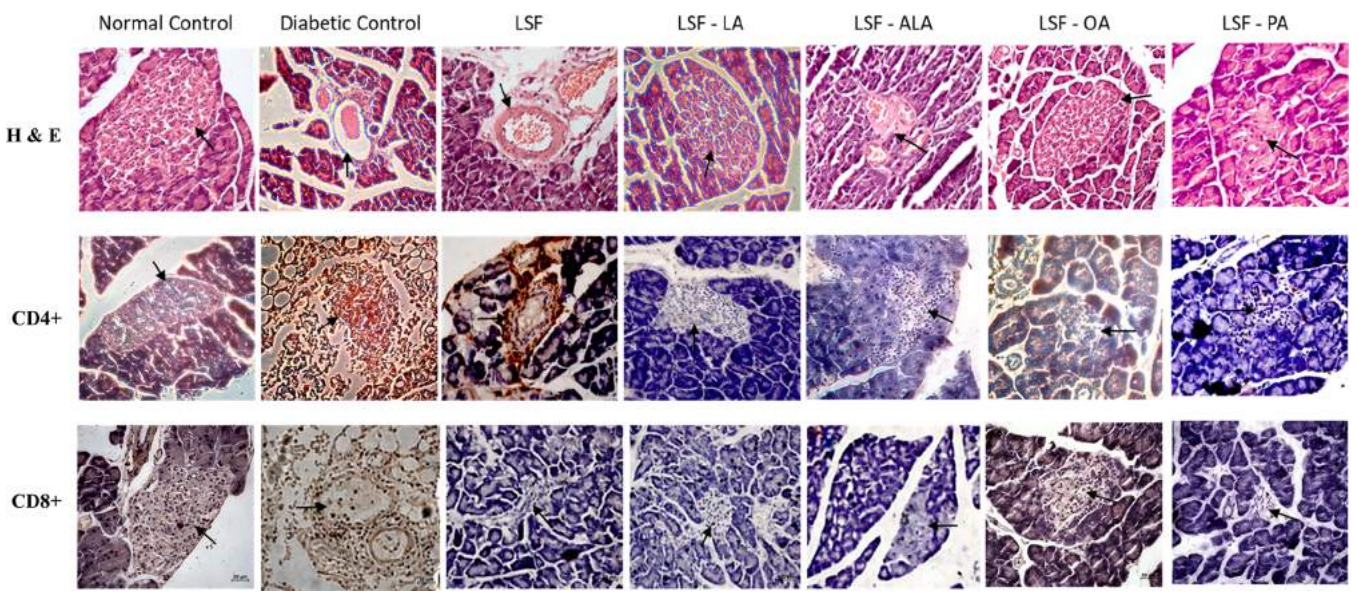

Figure 7. Immunohistochemical (IHC) study of pancreatic islets of control and treated groups after 35 days of treatment by hematoxylin-eosin (H&E) staining and expression of CD4+ and CD8+ T-cells (indicated by brown color and black arrows) (*under 400× magnification; 20 μm scale bar).

also showed a significant increase in FGL in 3rd and 5th weeks. LSF-LA and LSF-PA demonstrated a slight increase in FGL in the 5th week compared to their 3rd-week level. LSF-OA showed a better control of FGL than other prodrugs by maintaining a constant level throughout the study. In the LSF-ALA group, the FGL level exhibited a significant increase in the 5th week compared to the 3rd week (Figure 6A). All of the prodrugs showed significantly increased insulin levels compared to DC and free LSF groups (i.p.), among which LSF-OA and LSF-PA prodrugs showed higher insulin levels than LSF-LA and LSF-ALA, which indicates increased protection of the residual β cells owing to controlled blood glucose levels (Figure 6B).

In T1DM, progressive liver injury occurs due to an increase in oxidative stress, which is further associated with higher levels of SGOT (ASAT) and SGPT (ALAT) as seen in the DC

https://doi.org/10.1021/acs.jmedchem.1c00391
J. Med. Chem. XXXX, XXX, XXX−XXX

group. Treatment with the prodrugs lowered the levels of ALAT and ASAT, with minimum levels of ASAT being observed in LSF-OA and LSF-LA showed the lowest ALAT level. All of the groups exhibited similar total protein levels. Due to persistent hyperglycemia in the body, the renal functions get compromised, which increases the urea and uric acid levels in plasma. Here, all of the prodrugs showed a significant reduction in uric acid level compared to DC and free LSF with the highest reduction being observed in LSF-OA. It has also been reported that cholesterol and triglyceride levels are significantly increased in patients with diabetes due to insulin resistance and dyslipidemia. All of the prodrugs demonstrated a significant reduction in cholesterol and triglyceride levels compared to the DC group (Figure 6C).

Histopathology and Biochemical Assay. The pancreatic islets isolated after sacrificing the experimental animals at the terminal time point were analyzed for the morphology and immunohistochemical expression. The β-cells in DC were distorted, and very few of these were visible in islets after H&E staining compared to NC and other prodrugs. Although LSF, LSF-ALA, and LSF-PA exhibited proper arrangement of pancreatic islets, the number of β-cells were lesser compared to the LSF-LA- and LSF-OA-treated groups. A higher population of CD4+ and CD8+ inflammatory cells was seen in DC, along with the depletion of other cells in the vicinity. The presence of these inflammatory cells was significantly diminished in prodrug-treated diabetic rat's pancreas (Figure 7).

DISCUSSION AND CONCLUSIONS

LSF is a synthetic drug molecule that shows potent antidiabetic activity along with its well-known immunomodulatory and anti-inflammatory activities. To improve its physicochemical and pharmacokinetic attributes, we conjugated it with different types of FAs, which are also endogenously present in the human body and are synthesized by de novo lipogenesis of triglycerides and lipids. These are also extracted from plant and animal sources and are being consumed in diet and food supplements extensively. To reduce the solubility of hydrophilic LSF and to enhance its efficacy and bioavailability, we conjugated it with hydrophobic FAs belonging to different classes to form prodrugs with LSF with increased lipophilicity. LA has an 18-carbon chain and two double bonds (ω-6 FA; PUFA). OA also has an 18-carbon chain and is liquid in nature but with a single double bond (ω-9 FA; MUFA), which imparts fluidity to the cell membrane. SFA-like PA contains a 16-carbon chain without any double bond, making the cell membrane structure straight and rigid.[14] A functional short-chain FA, ALA, was also chosen for the study; it is a heterocyclic fatty acid derived from an octanoic acid.[15]

Here, the objective was to elucidate the effect of the length of carbon chain in terms of short and long chains, presence or absence of double bonds, and degree of unsaturation on the LSF-FA prodrug properties and associated pharmacological activity. In spite of same carbon chain length, FAs can demonstrate a huge difference in their physiological behavior owing to their geometrical and conformational differences.

FAs have been used in diabetes, mainly omega-3 FAs employed for the treatment of diabetes, particularly type 2 diabetes mellitus (T2DM), as these are known to decrease insulin resistance along with reducing the triglycerides levels in the body.[16] Here, FAs have been used as a carrier to deliver drug to increase its bioavailability and enhance the rate and extent of distribution inside the body. Previously, FAs like lauric acid and palmitic acid have been explored for the treatment of T2DM by conjugating with GLP-1 analogue, i.e., exendin-4, wherein pharmacokinetic parameters such as mean residence time and elimination $t_{1/2}$ were substantially improved compared with free exendin-4.[7] In another study, porcine zinc insulin was incorporated into mixed micelles of 30 mM bile salts and 40 mM linoleic acid for ileo-colonic delivery, and it exhibited 1.8% enhanced mean absolute bioavailability, leading to improved paracellular diffusion of the peptide.[17] As reported earlier by our group, LA conjugation to LSF also reduced the rapid conversion of LSF to PTX and increased the drug stability by offering protection to the hydroxyl group present in the side chain of LSF.[12] The nanosized micellar system generated due to the amphiphilic nature of prodrugs helps in bypassing the first-pass metabolism of LSF thus, increasing its bioavailability. It also enables RES escape prolonging its mean residence time in the body and reducing clearance.

First, LSF was synthesized in-house by reduction of the keto group of PTX using simple green chemistry followed by its purification. The synthesized drug was characterized by HPLC, FT-IR, and HR-MS analyses and compared with LSF procured from Cayman Chemical. The prodrugs were synthesized by conjugation of LSF with different categories of fatty acids LA, OA, PA, and ALA, all having the same structural chemistry (−COOH) at one end of carbon facilitating a similar procedure for the synthesis for all of the prodrugs. The mechanism is based on carbodiimide coupling, where FAs having free −COOH group was dissolved in DCM followed by the addition of 4-dimethylaminopyridine (DMAP) to activate the −COOH group, which forms an anhydride form of fatty acid.[18,19] Thereafter, the *N*-(3-dimethylaminopropyl)-*N*-ethyl-carbodiimide hydrochloride (EDC·HCl) was added into the ongoing reaction to form the *O*-acylisourea intermediate via an ion pair transfer; this *O*-acylisourea intermediate then reacted with the already present catalytic amount of DMAP (strong nucleophile) to form an acyl pyridinium specie, which acts as an acyl-transfer reagent and reacts with the −OH group of LSF to form ester linkage (−COOR′) between the fatty acid and LSF.[20] Herein, DMAP provided an appreciable yield of the product by preventing the formation of the byproduct (*N*-acylurea) during the reaction. This mechanism is also termed as the Steglich esterification. Then, the byproducts, unreacted EDC·HCl and DMAP, were washed out with water and brine solution (Figure 8).[21,22] There was a progressive increase in the hydrophobicity of the prodrugs as the alkyl chain length of the associated FA increased; this was reflected during the purification of the prodrugs in terms of the mobile phase ratio required and the elution time observed in flash chromatography; the same was further confirmed by the retention time of the prodrugs in HPLC (Table 1). The purified prodrugs also exhibited different physical states: LSF-LA and LSF-OA were in liquid form, while LSF-PA and LSF-ALA were solid in nature; this might be attributed to the presence of *cis* double bond in the long alkyl carbon chain of LA and OA that generates kinks and bents and does not allow the resultant molecules to attain a tightly packed structure.[23] The calculated molecular weight of all of the prodrugs matched with the molecular weight as obtained by HR-MS (Table 1). The proton NMR and FTIR spectra of prodrugs confirmed the removal of the −CH−OH group from 3360 cm^{-1} in FTIR and 3.9 ppm in NMR of LSF and the formation of $-CH-COO^{-}$ ester bond as revealed by signals at 2917−2933 cm^{-1} (FTIR)

https://doi.org/10.1021/acs.jmedchem.1c00391
J. Med. Chem. XXXX, XXX, XXX−XXX

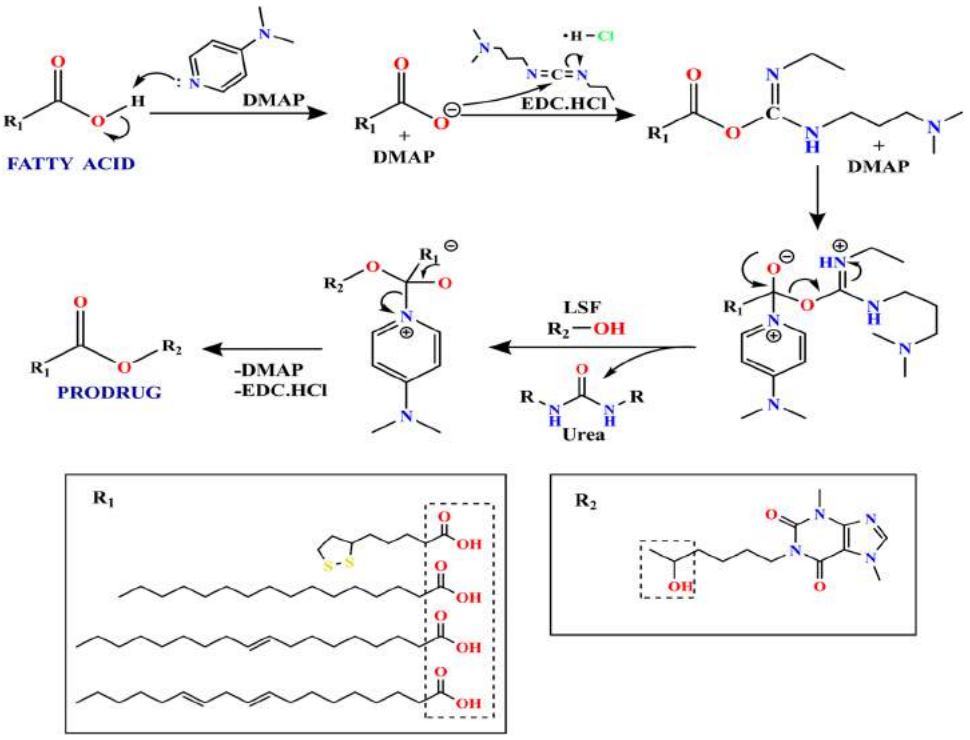

Figure 8. Mechanism involved in the formation of LSF−fatty acid prodrugs.

and 4.85−5 ppm (NMR, Figures S2−S6). The CMC value is important to determine the minimum media volume required to form micelles, wherein it depends on the hydrophobic chain length and varying structural properties of the compounds. It has been reported that with an increase in the carbon chain length, the CMC value decreases along with a low N_{agg}.[24,25] Aggregation number represents the average monomers involved in the formation of spherical micelles at or beyond CMC.[26] In our study, the nanosized self-assembled prodrugs showed CMC values ranging from 0.8 to 7.6 μg/mL, wherein LSF-LA exhibits CMC lower than LSF-ALA and LSF-PA owing to the longer chain length of LA, and LSF-OA has a higher CMC value due to a different degree of unsaturation compared to LSF-LA. LSF-ALA showed the least N_{agg}, which might be attributed to the short carbon chain of ALA, resulting in higher relative aqueous solubility in comparison to micelles of other prodrugs. A higher N_{agg} results in a low diffusion coefficient and reduced rate of transport from the interface to the bulk causing hindrance in the solubilization of the micelles. The prodrugs when evaluated for their stability and rate of release or cleavage of ester bond of free LSF from prodrugs in fresh rat plasma at 37 °C exhibited a sustained release of the drug up to 72 h (Figure 1), wherein 100% release of LSF was observed in the case of LSF-ALA, followed by other prodrugs in 72 h of the study. We did not observe a complete release of LSF in other prodrugs, that is, LSF-LA, LSF-PA, and LSF-OA owing to the following two reasons: (1) with every sample that is withdrawn, along with the drug, the LSF-FA prodrug also gets sampled out and thus is no longer available in the study to release the drug; this is an experimental limitation (the amount of drug getting sampled out as intact prodrug was also quantified in the case of LSF-ALA and LSF-OA (n = 4) and was found to be 0.98 ± 0.66% (observed only at 5 min time point) in LSF-ALA and 9.74 ± 2.3% (cumulative after 72 h) in LSF-OA). (2) Since plasma has been used here as the release media, the prodrugs and the released drug might have undergone metabolism. Overall, the experiment reconfirmed that conjugation of the FAs with small/large molecules enhances their *in vivo* stability in comparison to LSF.[27,28]

Adsorption and binding of the endogenous proteins on the surface of nanocarriers is a predominant factor affecting their behavior in the systemic circulation. To understand protein binding with the prodrugs, BSA was selected for the study owing to its structural similarity with human serum albumin (HSA) that is endogenously present and is majorly found in the circulatory system. It is well reported that the free FAs can easily bind to the HSA, which makes FAs and their conjugates potent and stable in the bloodstream.[29] Under normal physiological conditions, FA molecules bind to HSA in 1:1 or 1:2 ratio; this however increases by 4- to 5-fold under diabetic conditions,[8] further prolonging the mean residence time of the molecules in the circulation and thus supporting the choice of conjugating FAs with LSF to enhance its antidiabetic potential. The binding site per BSA molecule was found to be slightly higher in free LSF and LSF-ALA compared to other micelles, indicating lesser affinity of these micelles toward endogenous proteins in contrast to LSF-PA and LSF-OA micelles, which show higher binding affinity possibly due to the fact that FAs like OA and PA are abundantly present in the tissues and are known to bind firmly to albumin and use it as a carrier in the blood.[30] The *in vitro* study showed a lower binding constant of LSF-ALA followed by LSF-LA; however, LSF-OA and LSF-PA exhibited a stronger interaction with the protein (revealed by a higher value of binding constant and lower aggregation number), indicating a probable increase in half-life and mean residence time of the prodrugs and hence controlled release with prolonged availability of the drug *in vivo*.[31,32]

The proof of hemocompatibility of prodrugs was established by the *in vitro* study, wherein negligible hemolysis of RBCs was

https://doi.org/10.1021/acs.jmedchem.1c00391
J. Med. Chem. XXXX, XXX, XXX−XXX

observed in the presence of prodrug micelles (Figure 4A,B). PUFAs, especially are advantageous to the system because the presence of a long carbon chain increases the fluidity and flexibility of the membrane while maintaining the curvature of the membranes.[23,33] This was reflected in the higher cell uptake and internalization of the micelles of LSF-OA compared to other prodrugs and free LSF, signifying its optimum lipophilicity attributed due to the presence of a longer carbon chain followed by other prodrugs. Cell internalization of fatty acid-conjugated drug increases with an increase in the degree of lipophilicity of the prodrug, which is dictated by the chain length of fatty acid attached to LSF. As the chain length and degree of unsaturation of fatty acid increase, the extent and rate of cell internalization increase.[23] This is also reflected in the cellular uptake of LSF-ALA, which is almost similar to that of free LSF and minimum among all of the prodrugs attributed to its shorter carbon chain, rendering it less hydrophobic than other prodrugs and thus hindering its uptake. Further, this might have resulted in rapid cleavage of the ester bond in the growth media and release of free LSF before its internalization into the cells. Also, the prodrugs self-assembled into micelles, which offer the advantages of nanosize and thus exhibited a higher cell internalization compared to free drug.[5] Once the prodrugs are taken up by endocytosis, LSF gets cleaved from its fatty acid prodrug in the presence of acidic endosomal environment.[6] This further indicates that use of these FA-based prodrugs would enable a higher uptake of LSF into the cells as supported by the cell uptake data (Figure 4C) and greater therapeutic efficacy. The cell viability study of prodrug micelles in MIN-6 cells demonstrated a close to 100% cell viability in the presence of FAs as well as prodrugs (Figure 4D). Although some inflammatory effects of FAs have been reported earlier, such as PA exhibits increased apoptosis and cytotoxicity in HepG2 cells at 300 μM or higher concentrations;[34,35] however, these were found to be safe within the concentrations used in the present study. LSF prodrugs restored the cell viability in the presence of cytokines to a significant extent.

Conjugation of hydrophobic moieties like FAs to the drugs has been reported to improve the *in vivo* performance significantly by us as well as by other groups.[4,27,36,37] Conjugation of PA to the peptide, GLP-1 increased its $t_{1/2}$ from 5 min to 13 h providing it a sustained release.[28] Likewise, in this study, also the synthesized prodrugs exhibited 1.5- to 6-fold higher $t_{1/2}$ than free LSF with a simultaneous increase of 7- to 11-fold in MRT due to the increased hydrophobicity of the prodrugs attributed to the carbon chain present in FAs; MRT increases linearly with an increase in the chain length of the FA as shown in Table 4. The volume of distribution (V_d) of prodrugs was found to be higher than that of free LSF, wherein LSF-PA and LSF-OA demonstrated a 15 times higher V_d, indicating distribution to peripheral organs attributed to their longer chain length and hence greater lipophilicity.

In vivo efficacy of the prodrugs was evaluated in STZ-induced T1D model. The micelles used for treatment were formulated by the film hydration method and exhibited a particle size range of 70.4−170.5 nm with a narrow PDI. The FGL level was maintained at a significantly lower level than the diabetic control group in all of the treatment groups representing the antidiabetic potential of LSF but among all of the prodrugs, LSF-PA and LSF-OA showed the best control of glucose level with decreased mortality compared to other prodrugs (Figure 6A). Among all of the prodrugs, LSF-ALA exhibited a comparatively higher FGL, which might be due to the inadequate hydrophobicity of shorter carbon chain length of ALA affecting the half-life and MRT of LSF as seen in the PK data. A remarkable increase in the insulin level was found on the 21st day (3rd week) of the study, which further improved on the 35th day (5th week) in all of the prodrugs compared to the diabetic control and free LSF-treated group with LSF-OA treatment showing the highest insulin levels in comparison to the diabetic control group.

Persistent hyperglycemia induces certain adverse effects in kidney, pancreas, and other organs. A study of different biochemical parameters known to undergo a drastic change under diabetic conditions revealed that the prodrugs (particularly LSF-LA and LSF-OA) showed reduced oxidative stress as seen by the reduced plasma ASAT and ALAT levels compared to DC. Renal function also gets compromised in T1D as seen by the increased uric acid level in DC; LSF-OA showed a significantly reduced level of uric acid than other prodrugs. Diabetes can cause hepatic dyslipidemia, wherein low-density lipoproteins, total cholesterol, and triglycerides increase with a significant decrease in high-density lipoproteins; these stress-induced lipid metabolism changes are adequately addressed by the anti-inflammatory property of LSF.[38] LSF prodrugs treatment also reduced the total cholesterol and triglyceride levels rapidly after 21 days that was maintained till the 35th day of the study. There was no significant difference seen in total protein content in both DC and treatment groups.

The presence of proinflammatory cytokines induces the infiltration of CD4+ and CD8+ T lymphocytes in the pancreas causing destruction and depletion of β-cells in the islets in the diabetic model. The effectiveness of LSF released from the prodrugs in protecting the β-cells from inflammation and hence T-cell infiltration was shown by H&E and immunohistochemistry (IHC) staining of pancreatic tissues collected after 5 weeks of the treatment. H&E staining confirmed the intactness of β-cells in islets after treatment with the micelles of prodrugs compared to the diabetic control, most prominently visible in LSF-LA and LSF-OA prodrug-treated groups. Daily administration of LSF prodrugs also reduced the entry of T-cells (CD4+ and CD8+) into the islets, which otherwise cause β-cell destruction in comparison with the DC group (Figure 7).

The present study confirms the successful conjugation of LSF with different types of FAs and self-assembly into nanosized micelles along with improved *in vitro* and *in vivo* performance than the free drug itself. Among the different drug−FA prodrugs studied, LSF-OA showed comparatively better systemic pharmacokinetic and pharmacodynamic profiles in diabetes. OA, the fatty acid *per se*, has also been proven to be significantly better than PA in terms of its anti-inflammatory action, improved β-cell survival, and increased insulin sensitivity.[39]

LSF-OA exhibits greater and longer retention in the systemic circulation and efficiently treats diabetic condition with decreased mortality and stabilized FGL in diabetic Wistar rats. Overall, this research study presents OA as the most suitable FA among ALA, LA, PA, and OA for enhancing the stability and efficacy of LSF in diabetes treatment.

EXPERIMENTAL DESIGN

The synthesized LSF has >98% purity (Figure S7), whereas all of the prodrugs were found to be > 95% pure as revealed by HPLC analysis

https://doi.org/10.1021/acs.jmedchem.1c00391
J. Med. Chem. XXXX, XXX, XXX−XXX

(Figures S9−S12). All of the chemicals and reagents were of analytical grade with the highest possible purity purchased from commercial sources. MIN-6 cells were procured from NCCS, Pune (India). Wistar rats (male; 8−10 weeks, 200−220 g) were procured from Central Animal Facility, BITS-Pilani (Pilani, India). All animal experiments were performed in accordance with the guidelines laid down by CPCSEA, and the protocols were approved by Institutional Animal Ethics Committee (IAEC), BITS-Pilani.

Synthesis of LSF and LSF−Fatty Acid Prodrugs. LSF was synthesized in-house as reported earlier.[12] Briefly, in the presence of $NaBH_4$ (reducing agent) and protic solvent methanol, the carbonyl group present in the PTX was reduced to a secondary alcohol. The reaction mixture was stirred at room temperature, wherein the reaction progress was monitored by thin-layer chromatography (TLC; toluene/acetone ratio, 1:1). The resultant product, LSF, was characterized by HPLC, HR-MS, proton NMR, and FTIR analyses, and it was compared to the commercially available LSF (Cayman Chemical).

In brief, LSF was chemically conjugated to various FAs, namely, ALA, LA, PA, and OA to obtain prodrugs LSF-ALA, LSF-LA, LSF-PA, and LSF-OA, respectively (Scheme 1), using our previously reported method.[12] In brief, the coupling reaction of carbodiimide/DMAP was used to conjugate FAs to the LSF hydroxyl pendant group. At RT and under N_2, different FAs including ALA, LA, OA, and PA (21.6, 22, 19.2, and 21.1 mmol, respectively) were mixed with DMAP (1.2 equiv, 21.6 mmol) to form a uniform mixture in anhydrous dichloromethane (DCM) (250 mL), followed by the addition of EDC·HCl (1.5 equiv, 27 mmol); here, EDC has been used in its hydrochloride salt form to ensure its water solubility, which helps to remove the unreacted EDC during water workup in the postreaction step. To the reaction mixture, LSF (19.8 mmol) was added and left under stirring in the dark for the next 36 h. After completion of the reaction (as monitored by TLC using an ethyl acetate/hexane ratio of 90:10), the reaction mixture was washed twice with water and saturated solution of salt, dried over Na_2SO_4, and then DCM was evaporated under vacuum. The crude prodrugs so obtained from the above reaction were semisolid in texture. These crude prodrugs were then purified using flash chromatography (Bonna-Agela Technologies) using ethyl acetate/hexane as mobile phase in different ratios ranging from 45:55 to 95:5 depending upon the lipophilicity of the prodrug (Table S1). The instrumental parameters for all of the prodrugs were set constant; λ_{max} 273 nm and 20 mL/min flow rate using standard previously packed column (40 g; dimensions 3.1 cm × 14 cm) with silica gel (40−60 μm). A simple, rapid, and specific reversed-phase HPLC (RP-HPLC) method was developed for quantification of LSF[13] and LSF prodrugs. Briefly, for LSF quantification, chromatographic separation was performed on a UHPLC Thermo Fisher Scientific Inertsil ODS (C18) column (250 mm × 4.6 mm, 5 μm) with a mobile phase consisting of methanol/water (50:50% v/v) run in isocratic mode at a flow rate of 1 mL/min and detected at 273 nm. For the analysis of LSF-FA prodrugs, the mobile phase consisting of acetonitrile/sodium acetate buffer (10 mM; pH 3.5) in the ratio 95:05 was used by the chromatographic method given in Table 2. The analytical methods were validated for LSF-OA and LSF-ALA having the highest and least R_t according to the International Conference on Harmonization guideline Q2 (R1) with respect to selectivity, linearity, range, LOD, LOQ, precision, and assay. LOD and LOQ were determined by the signal-to-noise ratio method and further confirmed by the visual evaluation method. The purified prodrugs LSF-ALA, LSF-LA, LSF-PA, and LSF-OA were characterized for their physical appearance and by HPLC, HR-MS, ^{1}H NMR, and FTIR analyses.

Stability of Prodrugs in Plasma. Each prodrug was dissolved in dimethyl sulfoxide (DMSO) (20 mg/mL), and 10 μL of aliquot was spiked in rat plasma (2 mL) and maintained at 37 °C. At predetermined time points, 100 μL aliquots were withdrawn from each prodrug sample. To each of the aliquots, 50 μL of 3-isobutyl-1-methylxanthine (IBMX) (IS, 2 μg/mL) and 1.8 mL of DCM were added and mixed, which was then centrifuged at 3500 rpm and 4 °C for 15 min. The organic phase was then transferred into another tube, and DCM was evaporated under nitrogen stream. Using 200 μL of mobile phase, the dried samples were reconstituted and analyzed using our previously reported HPLC-based method.[13]

Self-Assembly of Prodrugs. The hydrophilic nature of LSF and the hydrophobic nature of FAs imparted an amphiphilic nature to all of the prodrugs, leading to their self-assembly into micelles. To study this, a solution of prodrugs in DCM was evaporated under vacuum to obtain a thin film, which was allowed to undergo self-assembly in aqueous media. The micelles so formed were sonicated for 3 min to enable size reduction. The size and ζ-potential were then recorded for all of the prodrug micelles with a scattering angle of 173° using a Zetasizer Nano-ZS (Malvern, U.K.).

CMC of Prodrugs. The self-assembling ability of the prodrugs was confirmed by fluorescence spectroscopy (RF-5301 Shimadzu, Japan). The CMC value of each prodrug was estimated using pyrene in aqueous solution. Pyrene dissolved in acetone (6×10^{-7} M) was incubated with different concentrations of prodrugs (1.0×10^{-5} to 1.0 mg/mL) and stirred at RT in the dark for 24 h. The fluorescence intensity of each sample was measured at an excitation range of 300−360 nm and emission at 390 nm with a slit width of 5 nm. The ratio of intensities of peaks at I_1 and I_3 corresponding to wavelengths 333 and 337 nm was recorded, and a graph was plotted between I_3 and I_1 versus log concentration of prodrugs.

Micelle Aggregation Number of the Prodrugs. Determination of micellar N_{agg} of prodrugs was performed by the fluorescence steady-state method at an excitation wavelength of 318 nm assuring that no Raman scattering will occur near the emission peaks projected from 320 nm to 450 nm at a 5 nm bandwidth. The probe and quencher (pyrene and CPC, respectively) were used here, wherein the sample preparation was done by dissolving pyrene (10^{-4} M) in 2 mL of ethanol, which was then evaporated under nitrogen, leaving out a thin film of pyrene.[26] The film was reconstituted into a 100 mL aqueous solution of prodrug micelles at a 30 times CMC value of the respective prodrug, with overnight stirring at RT (solution 1, 2×10^{-6} M pyrene in 100 mL of micellar solution). Solution 2 was prepared by taking 110.05 mg of CPC in 10 mL of solution 1 (CPC concentration, 2.8×10^{-3} M). The molar concentration of quencher was further varied from 0 to 1.12×10^{-3} M by diluting it with solution 1, and probe intensities were thereafter recorded.

$$\ln \frac{F_0}{F_Q} = \frac{Q}{M} \tag{1}$$

where

$$M = \frac{C - \mathrm{CMC}}{N_{agg}} \tag{2}$$

Here, M is the micellar concentration, F_Q and F_0 are the fluorescence intensities of probe with and without quencher, respectively, Q is the concentration of quencher in micelle solution, C is the concentration of prodrug, CMC is the critical micelle concentration of prodrug, and N_{agg} is the aggregation number.

Protein Interaction of Prodrug Micelles. BSA was selected here as a model protein which undergoes a change in its UV absorption spectra when incubated with different concentrations of prodrug micelles. With the help of the fluorescence quenching method, the change in fluorescence spectra of the protein was recorded after incubating it with micelles using the Scatchard equation (eq 3). Binding site present per BSA molecule represents the prodrug binding on the vacant sites of the protein.

$$\log \frac{F_0 - F_Q}{F_Q} = \log K_b + n \log[Q] \tag{3}$$

where F_0 and F_Q as in the above formula represent the fluorescence intensities in the absence and presence of quencher at any particular concentration (Q), respectively, n denotes the number of binding sites per protein molecule, and K_b is the apparent biding constant.

Preparation of samples was done by producing a series of different concentrations of prodrug micelles (0−100 μM) and spiking with a

https://doi.org/10.1021/acs.jmedchem.1c00391
J. Med. Chem. XXXX, XXX, XXX−XXX

constant amount of BSA (2 μM). Fluorescence intensities were recorded after 30 min of incubation of each sample at excitation and emission wavelengths of 280 and 343 nm, respectively. For the determination of the number of binding sites and binding constant, a graph was plotted between $\log(F_0 - F_Q)/F_Q$ and log of quencher concentration (LSF or prodrug). Further, the mechanism of quenching of BSA molecule by LSF or prodrug was studied by a UV−visible spectrophotometer (JASCO V-650) using a quartz cell having 1 cm path length.

***In Vitro* Cell Culture Studies of Self-Assembled Micelles of the LSF−Fatty Acid Prodrugs.** The efficacy of LSF prodrug micelles was evaluated in MIN-6 cells. These cells were cultured in DMEM supplemented with 10% FBS and incubated in 5% CO_2 at 37 °C.

***In Vitro* Hemocompatibility Study.** The interaction of prodrug micelles with blood was studied *in vitro* with modification in the previously reported method.[40] Blood was collected from Wistar rats and mixed with ethylenediamine tetraacetic acid (EDTA) solution (10% w/v) to prevent coagulation. It was washed three times with normal saline solution followed by centrifugation at 1500 rpm for 10 min at 4 °C. The RBCs so obtained were then diluted in a 1:5 ratio with normal saline solution. Free LSF (20 μM) and prodrug micelles (~20 μM LSF) were dispersed in 1 mL of RBC suspension with negative and positive control groups (normal saline and 0.1% Triton X solution, respectively). After incubation for 1 h at 37 °C, each sample was centrifuged at 2000 rpm for 5 min and 200 μL of the supernatant was analyzed for optical density (OD) at 540 nm using an Epoch microplate spectrophotometer (BioTek Instruments, VT). The percentage hemolysis was determined using eq 4.

$$\%\text{hemolysis} = \frac{\text{OD}_{\text{sample}} - \text{OD}_{\text{negative control}}}{\text{OD}_{\text{positive control}} - \text{OD}_{\text{negative control}}} \times 100 \quad (4)$$

Cell Internalization of Prodrug Micelles. The internalization of free drug and micelles of self-assembled LSF prodrugs into the cells was studied. In this study, MIN-6 cells (2×10^4 cells/per well) were plated and incubated in 5% CO_2 at 37 °C till confluency has reached. After 24 h, the cells were treated with micelles of all of the four types of prodrugs (~20 μM free LSF) and free LSF (20 μM) and incubated for 6 h. The cells without treatment served as the negative control. After incubation, media was collected followed by washing the cells twice with phosphate-buffered saline (PBS) before scrapping off cells in PBS solution. Extraction of the prodrugs and LSF from the media and washing the solution and cell lysates was carried out using DCM (1.3 mL) followed by centrifugation at 3500 rpm. DCM was transferred in a fresh tube and dried under nitrogen. The residue was then redispersed into 200 μL of mobile phase and analyzed for LSF/prodrugs by HPLC.

Cell Viability Assay (under Normal and Inflammatory Conditions). MIN-6 cells (5000 cells/well) were seeded and allowed to adhere for 24 h in a 96-well culture plate under normal growth conditions. Different treatments were given to the cells including the prodrug micelles, free LSF, and free fatty acids (LA, OA, PA, and ALA) at 20 μM concentration and incubated at 37 °C. The cells incubated in growth media only served as the negative control, while the cells incubated with a cocktail of three different proinflammatory cytokines (TNF-α; 10 ng/mL, IL-1β; 5 ng/mL and IFN-γ; 100 ng/mL) served as the positive control.[41] After 48 h, 3-[4,5-dimethylthiazol-2-yl]-2,5-diphenyltetrazolium bromide (MTT) assay was performed and the inhibition in cell growth was determined with respect to untreated cells (media only).[42]

$$\%\text{cell viability} = \frac{\text{absorbance}_{\text{sample wells}}}{\text{absorbance}_{\text{untreated wells}}} \times 100 \quad (5)$$

Once the cell compatibility was confirmed, freshly seeded MIN-6 cells (5000 cells/well) were further exposed to the above-mentioned mixture of proinflammatory cytokines to induce inflammation[43] followed by treatment with free LSF and synthesized LSF prodrugs (~20 μM free LSF). After 48 h, cell viability was analyzed by MTT assay recording absorbance at 560 and 630 nm followed by calculating the % cell viability using eq 5.

***In Vivo* Evaluation of Prodrugs.** All of the experiments were carried out in compliance with CPCSEA guidelines, and protocols were approved by IAEC, BITS-Pilani, Pilani. The rats were housed in well-ventilated cages with periodic light/dark periods for 12 h and fed within standard laboratory conditions with routine *ab libitum* diet.

Systemic Pharmacokinetics of Prodrug. The micelles of LSF prodrugs and free LSF were injected intravenously into the Wistar rats (200−220 g) at doses of 30 mg/kg (~15 mg/kg of LSF) and 15 mg/kg, respectively. Blood samples were collected by the retro-orbital route at preset time points till 24 h. Plasma was retrieved from the collected blood followed by sample extraction and sample analysis (previously described in the Stability of Prodrugs in Plasma section). Using noncompartmental model, plasma concentration−time profile was plotted for free LSF and its prodrugs employing Phoenix 2.1 WinNonlin (Pharsight Corporation).

Efficacy Studies in STZ-Induced T1DM Model. STZ-induced diabetes model was created in Wistar rats (200−220 g) with a standard dose of STZ (55 mg/kg) prepared in cold citrate buffer (0.01 M, pH 4.5) using the i.p. route, while control rats were administered only buffer. Fasting glucose level was measured after 72 h of STZ injection, and animals exhibiting a plasma glucose level of 250 mg/dL or greater were labeled as diabetic. The rats were randomly grouped into NC, DC, free LSF-treated, and self-assembled prodrug micelles treated rats. Treatment was initiated on the 3rd day after the hyperglycemic state was verified.

For the daily treatment regimen, one of the groups was treated with 15 mg/kg i.p. injection of free LSF solution in water. The self-assembled micelles of the respective four prodrugs were delivered at 30 mg/kg dose (~15 mg/kg of free LSF) once daily to each of the groups. The blood glucose levels were measured using an Accu-Check active glucometer by the tail bleeding method on every 3rd day till 5 weeks. Plasma was collected after 21 and 35 days and used for estimating the insulin levels and biochemical parameters for lipid and protein profiling of liver and kidney functions.

Histopathology and Immunohistochemical Analysis. After giving treatment to the animals for 5 weeks, they were sacrificed for the assessment of pancreatic islet morphology with the help of H&E staining. Standard protocol was followed for IHC analysis of the expression of CD4+ and CD8+ T-cells in the pancreatic samples. The primary antibodies used were CD4 Rabbit mAb (1:400) and CD8a Mouse mAb (1:20). As a secondary antibody, signal stain IHC boost reagent and anti-mouse IgG antibody were used at 1:1 and 1:500 dilutions, respectively.

Statistical Analysis. All of the data have been expressed as mean ± standard deviation and analyzed using GraphPad Prism 7.0 software (GraphPad Software, San Diego, CA). Statistical analysis was performed using one-way ANOVA by Tukey's multiple comparison test with a 95% confidence interval for confirming the difference between the groups. A p-value < 0.05 was considered statistically significant.

■ ASSOCIATED CONTENT

Supporting Information

The Supporting Information is available free of charge at https://pubs.acs.org/doi/10.1021/acs.jmedchem.1c00391.

Characterization of LSF and all its prodrugs by spectrometric methods: NMR, mass, FTIR, and purity chromatograms by the HPLC method; stacked ^{1}H NMR of LSF and prodrugs in $CDCl_3$ solvent (Figure S1); NMR characterization of Lisofylline (LSF) (Figure S2); NMR characterization of LSF-LA prodrug (Figure S3); NMR characterization of LSF-ALA prodrug (Figure S4); NMR characterization of LSF-OA prodrug (Figure S5); NMR characterization of LSF-PA prodrug (Figure S6); HPLC purity spectra of synthesized LSF (Figure S7); stacked representative HPLC chromatograms of LSF

https://doi.org/10.1021/acs.jmedchem.1c00391
J. Med. Chem. XXXX, XXX, XXX−XXX

prodrugs (Figure S8); HPLC purity spectra of LSF-LA prodrug (Figure S9); HPLC purity spectra of LSF-ALA prodrug (Figure S10); HPLC purity spectra of LSF-OA prodrug (Figure S11); HPLC purity spectra of LSF-PA prodrug (Figure S12); stacked mass spectra of LSF prodrugs (Figure S13); stacked FTIR spectra of LSF prodrugs (Figure S14); optimized mobile phase ratio for purifying prodrugs using flash chromatography (Table S1); precision (% RSD) and accuracy (% bias) of analytical methods of LSF prodrugs LSF-ALA and LSF-OLA (Table S2); and precision and accuracy of quality control (QC) samples of LSF prodrugs (Table S3) (PDF).

SMILES of the drug compounds (CSV)

AUTHOR INFORMATION

Corresponding Author

Anupama Mittal − *Department of Pharmacy, Birla Institute of Technology and Science (BITS PILANI), Pilani, Rajasthan 333031, India;* orcid.org/0000-0003-3344-9579; Phone: +911596 255708; Email: anupama.mittal@pilani.bits-pilani.ac.in

Authors

Arihant Kumar Singh − *Department of Pharmacy, Birla Institute of Technology and Science (BITS PILANI), Pilani, Rajasthan 333031, India;* orcid.org/0000-0002-9659-5998

Kishan S. Italiya − *Department of Pharmacy, Birla Institute of Technology and Science (BITS PILANI), Pilani, Rajasthan 333031, India*

Saibhargav Narisepalli − *Department of Pharmacy, Birla Institute of Technology and Science (BITS PILANI), Pilani, Rajasthan 333031, India*

Deepak Chitkara − *Department of Pharmacy, Birla Institute of Technology and Science (BITS PILANI), Pilani, Rajasthan 333031, India;* orcid.org/0000-0003-4174-7664

Complete contact information is available at: https://pubs.acs.org/10.1021/acs.jmedchem.1c00391

Notes

The authors declare no competing financial interest.

ACKNOWLEDGMENTS

The work elaborated in the study was funded by SERB-DST, Govt. of India research grant #YSS/2014/000551.

ABBREVIATIONS USED

^{1}H NMR, proton nuclear magnetic resonance spectroscopy; ALA, α-lipoic acid; BSA, bovine serum albumin; $CDCl_3$, deuterated chloroform; CMC, critical micellar concentration; CPC, cetylpyridinium chloride; Cyt, cytokines; DC, diabetic control; DM, diabetes mellitus; DMAP, 4-dimethylaminopyridine; DMSO, dimethyl sulfoxide; EDC·HCl, *N*-(3-dimethylaminopropyl)-*N*-ethylcarbodiimide hydrochloride; EDTA, ethylenediamine tetraacetic acid; FA, fatty acid; FGL, fasting glucose level; FTIR, Fourier transform infrared spectroscopy; H&E, hematoxylin and eosin; HPLC, high-performance liquid chromatography; HR-MS, high-resolution mass spectroscopy; HSA, human serum albumin; i.p, intraperitoneal route; IBMX, 3-isobutyl-1-methylxanthine; IHC, immunohistochemical; LA, linoleic acid; LSF, lisofylline; MIN-6, mouse insulinoma cells; MRT, mean residence time; MTT, (3-[4,5-dimethylthiazol-2-yl]-2,5-diphenyltetrazolium bromide; MUFA, monounsaturated fatty acid; N_{agg}, aggregation number; NC, normal control; OA, oleic acid; OD, optical density; PA, palmitic acid; PK, pharmacokinetic; PTX, pentoxifylline; PUFA, polyunsaturated fatty acid; RBC, red blood cell; R_t, retention time; SFA, saturated fatty acid; STZ, streptozotocin; T1DM, type 1 diabetes mellitus; T2DM, type 2 diabetes mellitus; TLC, thin-layer chromatography; USFA, unsaturated fatty acid; V_d, volume of distribution; ω-6, omega-6; ω-9, omega-9

REFERENCES

(1) Chen, M.; Yang, Z.; Wu, R.; Nadler, J. L. Lisofylline, a novel antiinflammatory agent, protects pancreatic beta-cells from proinflammatory cytokine damage by promoting mitochondrial metabolism. *Endocrinology* **2002**, *143*, 2341−2348.

(2) Jung, H. J.; Ho, M. J.; Ahn, S.; Han, Y. T.; Kang, M. J. Synthesis and physicochemical evaluation of entecavir-fatty acid conjugates in reducing food effect on intestinal absorption. *Molecules* **2018**, *23*, No. 731.

(3) Irby, D.; Du, C.; Li, F. Lipid−drug conjugate for enhancing drug delivery. *Mol. Pharmaceutics* **2017**, *14*, 1325−1338.

(4) Bradley, M. O.; Webb, N. L.; Anthony, F. H.; Devanesan, P.; Witman, P. A.; Hemamalini, S.; Chander, M. C.; Baker, S. D.; He, L.; Horwitz, S. B. Tumor targeting by covalent conjugation of a natural fatty acid to paclitaxel. *Clin. Cancer Res.* **2001**, *7*, 3229−3238.

(5) Uppal, S.; Italiya, K. S.; Chitkara, D.; Mittal, A. Nanoparticulate-based drug delivery systems for small molecule anti-diabetic drugs: an emerging paradigm for effective therapy. *Acta Biomater.* **2018**, *81*, 20−42.

(6) Li, F.; Snow-Davis, C.; Du, C.; Bondarev, M. L.; Saulsbury, M. D.; Heyliger, S. O. Preparation and characterization of lipophilic doxorubicin pro-drug micelles. *J. Vis. Exp.* **2016**, No. 54338.

(7) Chae, S. Y.; Choi, Y. G.; Son, S.; Jung, S. Y.; Lee, D. S.; Lee, K. C. The fatty acid conjugated exendin-4 analogs for type 2 antidiabetic therapeutics. *J. Controlled Release* **2010**, *144*, 10−16.

(8) Elsadek, B.; Kratz, F. Impact of albumin on drug delivery-new applications on the horizon. *J. Controlled Release* **2012**, *157*, 4−28.

(9) Fattahi, N.; Shahbazi, M.-A.; Maleki, A.; Hamidi, M.; Ramazani, A.; Santos, H. A. Emerging insights on drug delivery by fatty acid mediated synthesis of lipophilic prodrugs as novel nanomedicines. *J. Controlled Release* **2020**, *326*, 556−598.

(10) Fattahi, N.; Bahari, A.; Ramazani, A.; Koolivand, D. In vitro immunobiological assays of methotrexate-stearic acid conjugate in human PBMCs. *Immunobiology* **2020**, *225*, No. 151984.

(11) Fattahi, N.; Ayubi, M.; Ramazani, A. Amidation and esterification of carboxylic acids with amines and phenols by N, N′-diisopropylcarbodiimide: a new approach for amide and ester bond formation in water. *Tetrahedron* **2018**, *74*, 4351−4356.

(12) Italiya, K. S.; Mazumdar, S.; Sharma, S.; Chitkara, D.; Mahato, R. I.; Mittal, A. Self-assembling lisofylline-fatty acid conjugate for effective treatment of diabetes mellitus. *Nanomedicine* **2019**, *15*, 175−187.

(13) Italiya, K. S.; Sharma, S.; Kothari, I.; Chitkara, D.; Mittal, A. Simultaneous estimation of lisofylline and pentoxifylline in rat plasma by high performance liquid chromatography-photodiode array detector and its application to pharmacokinetics in rat. *J. Chromatogr. B* **2017**, *1061−1062*, 49−56.

(14) Nagy, K.; Tiuca, I.-D. Importance of Fatty Acids in Physiopathology of Human Body. In *Fatty Acids*; Catala, A., Ed.; IntechOpen: 2017; pp 3−22.

(15) Seifar, F.; Khalili, M.; Khaledyan, H.; Amiri Moghadam, S.; Izadi, A.; Azimi, A.; Shakouri, S. K. α-Lipoic acid, functional fatty acid, as a novel therapeutic alternative for central nervous system diseases: A review. *Nutr. Neurosci.* **2019**, *22*, 306−316.

(16) Sobczak, A. I. S.; Blindauer, C. A.; Stewart, J. A. Changes in plasma free fatty acids associated with type-2 diabetes. *Nutrients* **2019**, *11*, No. 2022.
(17) Scott-Moncrief, J. C.; Shao, Z.; Mitra, A. K. Enhancement of intestinal insulin absorption by bile salt−fatty acid mixed micelles in dogs. *J. Pharm. Sci.* **1994**, *83*, 1465−1469.
(18) Ramazani, A.; Nasrabadi, F. Z.; Rezaei, A.; Rouhani, M.; Ahankar, H.; Asiabi, P. A.; Joo, S. W.; Ślepokura, K.; Lis, T. Synthesis of N-acylurea derivatives from carboxylic acids and N, N′-dialkyl carbodiimides in water. *J. Chem. Sci.* **2015**, *127*, 2269−2282.
(19) Fattahi, N.; Triantafyllidis, K.; Luque, R.; Ramazani, A. Zeolite-based catalysts: a valuable approach toward ester bond formation. *Catalysts* **2019**, *9*, No. 758.
(20) Fattahi, N.; Ramazani, A.; Kinzhybalo, V. Imidazole-functionalized Fe 3 O 4/chloro-silane core-shell nanoparticles: an efficient heterogeneous organocatalyst for esterification reaction. *Silicon* **2019**, *11*, 1745−1754.
(21) Tsakos, M.; Schaffert, E. S.; Clement, L. L.; Villadsen, N. L.; Poulsen, T. B. Ester coupling reactions−an enduring challenge in the chemical synthesis of bioactive natural products. *Nat. Prod. Rep.* **2015**, *32*, 605−632.
(22) Fattahi, N.; Varnaseri, N.; Ramazani, A. A novel approach toward thioester bond formation mediated by N, N′-diisopropylcarbodiimide in water. *Phosphorus, Sulfur Silicon Relat. Elem.* **2021**, *196*, 6−12.
(23) De Carvalho, C. C.; Caramujo, M. J. The various roles of fatty acids. *Molecules* **2018**, *23*, No. 2583.
(24) Mahmood, M. E.; Al-Koofee, D. A. Effect of temperature changes on critical micelle concentration for tween series surfactant. *Glob. J. Sci. Front. Res. Chem.* **2013**, *13*, 1−7.
(25) Luan, H.; Gong, L.; Yue, X.; Nie, X.; Chen, Q.; Guan, D.; Que, T.; Liao, G.; Su, X.; Feng, Y. Micellar aggregation behavior of alkylaryl sulfonate surfactants for enhanced oil recovery. *Molecules* **2019**, *24*, No. 4325.
(26) Turro, N. J.; Yekta, A. Luminescent probes for detergent solutions. A simple procedure for determination of the mean aggregation number of micelles. *J. Am. Chem. Soc.* **1978**, *100*, 5951−5952.
(27) Sloat, B. R.; Sandoval, M. A.; Li, D.; Chung, W.-G.; Lansakara-P, D. S.; Proteau, P. J.; Kiguchi, K.; DiGiovanni, J.; Cui, Z. In vitro and in vivo anti-tumor activities of a gemcitabine derivative carried by nanoparticles. *Int. J. Pharm.* **2011**, *409*, 278−288.
(28) Agersø, H.; Jensen, L.; Elbrønd, B.; Rolan, P.; Zdravkovic, M. The pharmacokinetics, pharmacodynamics, safety and tolerability of NN2211, a new long-acting GLP-1 derivative, in healthy men. *Diabetologia* **2002**, *45*, 195−202.
(29) Curry, S.; Brick, P.; Franks, N. P. Fatty acid binding to human serum albumin: new insights from crystallographic studies. *Biochim. Biophys. Acta, Mol. Cell Biol. Lipids* **1999**, *1441*, 131−140.
(30) Spector, A. A.; John, K.; Fletcher, J. E. Binding of long-chain fatty acids to bovine serum albumin. *J. Lipid Res.* **1969**, *10*, 56−67.
(31) Keller, F.; Maiga, M.; Neumayer, H.-H.; Lode, H.; Distler, A. Pharmacokinetic effects of altered plasma protein binding of drugs in renal disease. *Eur. J. Drug Metab. Pharmacokinet.* **1984**, *9*, 275−282.
(32) Yu, X.; Liu, R.; Ji, D.; Yang, F.; Li, X.; Xie, J.; Zhou, J.; Yi, P. Study on the synergism effect of lomefloxacin and ofloxacin for bovine serum albumin in solution by spectroscopic techniques. *J. Solution Chem.* **2011**, *40*, 521−531.
(33) Pinot, M.; Vanni, S.; Pagnotta, S.; Lacas-Gervais, S.; Payet, L.-A.; Ferreira, T.; Gautier, R.; Goud, B.; Antonny, B.; Barelli, H. Polyunsaturated phospholipids facilitate membrane deformation and fission by endocytic proteins. *Science* **2014**, *345*, 693−697.
(34) Sharma, R. B.; Alonso, L. C. Lipotoxicity in the pancreatic beta cell: not just survival and function, but proliferation as well? *Curr. Diabetes Rep.* **2014**, *14*, No. 492.
(35) Luo, Y.; Rana, P.; Will, Y. Palmitate increases the susceptibility of cells to drug-induced toxicity: an in vitro method to identify drugs with potential contraindications in patients with metabolic disease. *Toxicol. Sci.* **2012**, *129*, 346−362.
(36) Wu, L.; Zhang, F.; Chen, X.; Wan, J.; Wang, Y.; Li, T.; Wang, H. Self-assembled gemcitabine prodrug nanoparticles show enhanced efficacy against patient-derived pancreatic ductal adenocarcinoma. *ACS Appl. Mater. Interfaces* **2020**, *12*, 3327−3340.
(37) Breistøl, K.; Balzarini, J.; Sandvold, M. L.; Myhren, F.; Martinsen, M.; De Clercq, E.; Fodstad, O. Antitumor activity of P-4055 (elaidic acid-cytarabine) compared to cytarabine in metastatic and sc human tumor xenograft models. *Cancer Res.* **1999**, *59*, 2944−2949.
(38) Bursten, S. L.; Federighi, D.; Wald, J.; Meengs, B.; Spickler, W.; Nudelman, E. Lisofylline causes rapid and prolonged suppression of serum levels of free fatty acids. *J. Pharmacol. Exp. Ther.* **1998**, *284*, 337−345.
(39) Nemecz, M.; Constantin, A.; Dumitrescu, M.; Alexandru, N.; Filippi, A.; Tanko, G.; Georgescu, A. The distinct effects of palmitic and oleic acid on pancreatic beta cell function: the elucidation of associated mechanisms and effector molecules. *Front. Pharmacol.* **2019**, *9*, No. 1554.
(40) Sharma, S.; Mazumdar, S.; Italiya, K. S.; Date, T.; Mahato, R. I.; Mittal, A.; Chitkara, D. Cholesterol and morpholine grafted cationic amphiphilic copolymers for miRNA-34a delivery. *Mol. Pharmaceutics* **2018**, *15*, 2391−2402.
(41) Wu, J. J.; Chen, X.; Cao, X.-C.; Baker, M. S.; Kaufman, D. B. Cytokine-induced metabolic dysfunction of MIN6 β cells is nitric oxide independent. *J. Surg. Res.* **2001**, *101*, 190−195.
(42) Italiya, K. S.; Singh, A. K.; Chitkara, D.; Mittal, A. Nanoparticulate tablet dosage form of lisofylline-linoleic acid conjugate for Type 1 diabetes: in situ single-pass intestinal perfusion (SPIP) studies and pharmacokinetics in rat. *AAPS PharmSciTech* **2021**, *22*, No. 114.
(43) Cui, P.; Macdonald, T. L.; Chen, M.; Nadler, J. L. Synthesis and biological evaluation of lisofylline (LSF) analogs as a potential treatment for type 1 diabetes. *Bioorg. Med. Chem. Lett.* **2006**, *16*, 3401−3405.

https://doi.org/10.1021/acs.jmedchem.1c00391
J. Med. Chem. XXXX, XXX, XXX−XXX